IEEE Access
Multidisciplinary | Rapid Review | Open Access Journal

Received 11 January 2023, accepted 25 January 2023, date of publication 30 January 2023, date of current version 2 February 2023.

Digital Object Identifier 10.1109/ACCESS.2023.3240660

RESEARCH ARTICLE

EWMA Control Chart for Rayleigh Process With Engineering Applications

FUAD S. ALDUAIS[1,2] **AND ZAHID KHAN**[3]

[1]Department of Mathematics, College of Science and Humanities in Al-Kharj, Prince Sattam bin Abdulaziz University, Al-Kharj 11942, Saudi Arabia
[2]Administration Department, Administrative Science College, Thamar University, Thamar, Yemen
[3]Department of Mathematics and Statistics, Hazara University Mansehra, Mansehra 21120, Pakistan

Corresponding author: Fuad S. Alduais (f.alduais@psau.edu.sa)

This work was supported by Prince Sattam bin Abdulaziz University under Project PSAU/2022/01/21867.

ABSTRACT Process monitoring is typically performed with quality control charts. The normality assumption is often taken into consideration for the development of control charts. However, this assumption may not hold in many real-life situations. One such circumstance is utilizing the V_{SQR} chart to track the process variability of Rayleigh distributed processes. The structure of the V_{SQR} chart follows the basic design of the Shewhart-type chart, which is not sensitive mainly for smaller to moderate shifts in monitoring parameter. In this paper, an enhanced approach, namely Rayleigh exponential weighted moving average (REWMA) is introduced. The suggested REWMA scheme aims to significantly improve the detection capabilities of the traditional V_{SQR} chart. Designated limits, along with charting parameters, are evaluated for different sample sizes. The effectiveness of the suggested REWMA control chart is assessed in terms of run length distributional parameters. Moreover, the Monte Carlo simulations are made to compare the run length properties of the proposed REWMA chart with the existing competitor design. The comparative assessment demonstrates that the suggested offers a considerable enhancement relative to the competing design. An application of the REWMA chart on simulated data also reveals that the proposed chart is highly sensitive to smaller and persistent shifts in the scaling parameter of Rayleigh distribution. Finally, an example from real-life has been presented to illustrate the importance of the suggested chart.

INDEX TERMS Rayleigh distribution, estimation, control chart, non-normal process, EWMA chart, simulation.

I. INTRODUCTION

In industrial production processes, statistical process control (SPC) offers a variety of control charts for tracking abrupt changes in parameters of quality characteristics [1]. This method is commonly employed, notably in the service, chemical industries, and manufacturing sectors to keep quality tabs on production or manufacturing operations [2]. Managerial framework in advanced industrial sectors is making use of SPC's helpful features to boost the quality of their products [3]. Fundamentally, SPC is a collection of tools for improving process stability, efficiency, and product quality by identifying and tracking irregular fluctuations in a manufacturing process [4]. In contrast, the control chart within the SPC is the primary inspection technique for minimizing production-line fluctuations. The primary goal of employing a control chart is to determine abnormal changes in a process as early as possible, hence preventing the production of faulty products [5]. Monitoring a process is seen as a continuous process that demands careful evaluation in order to achieve improved output quality. Monitoring and spotting the usual occurrences helps improve product quality and improve process productivity [6], [7], [8]. Control charts make it easier to distinguish between unnatural and natural fluctuations, which lower the amount of scrap produced [9]. Timely identification of changes that occur in a steady process is required, and dispersion and location are crucial elements in this regard [10]. Control charts were initially presented by Shewhart in 1926, and since then, they have been employed in several production processes [11].

The associate editor coordinating the review of this manuscript and approving it for publication was Sajid Ali.

Even though Shewhart control charts are easy to utilize and very effective at finding major changes in study parameters, they are not capable of detecting small or moderate shifts [12]. However, memory-type charts, particularly EWMA chart, MA chart, and CUSUM chart have incredible performance in terms of faster respond on process shifts since their plotting statistics rely on both past and current information. Most studies on traditional designing control charts are premised on the assumption that the underlying processes are normal. This assumption, however, may not be tenable for some real-life quality processes. If the underlying quality characteristics are not normally distributed, the typical methods of chart designing may not be adequate and their applications lead to invalid decisions [13], [14], [15], [16]. In this regard, non-normality-based monitoring schemes have recently drawn a lot of research interest. For instance, using the premise that the observed variable followed the log-normal, Weibull, and gamma models, a monitoring scheme has been designed in [17]. An exponential distribution-based t-chart has been proposed by Santiago and Smith [18]. The percentiles-based charting design relied on the Gumbel distribution studied by Rosaiah et al. [19]. Hossain, Omar, and Riaz developed the V chart for Rayleigh quality characteristics [18]. A charting design in the case of type II censoring data under Weibull model has been suggested by Hossain et al. [20].The Weibull model-based design for type-II censoring and complete data was proposed by Guo et al. [21]. Wang et al. [22] and Khan et al. have made additional developments using the Rayleigh distribution as an acceptable model for industrial variables [23], [24].The other most updated references on nonnormal processes in respect to Shewhart type designs can be seen in [25].There are also many non-parametric graphical charts have been developed to handle the distribution free data [26].

The EWMA monitoring scheme for non-normal heavy-tailed distributions, including skewed distributions, has been described by Borror et al. [27]. The authors conducted the simulation experiment to determine the average run length (ARL) distribution for the EWMA control chart's performance and concluded that it is robust for violations of the normality assumption. For the asymmetric processes, Alkahtani [28] investigated the behavior of double EWMA and EWMA control charts. The transformation approach for calculating the time between data points, as proposed by Montgomery [29] may be utilized. The transformed exponential distribution and Weibull distribution are examined by Liu et al. [30] in the robust framework for cumulative quality control and EWMA chart. Although non-normality-based control charts have been widely investigated in the literature, their design for specific quality characteristics needs more exploration.

This research is an effort to provide an improved monitoring scheme for Rayleigh distributed processes. Rapid response to any changes in the process parameters and subsequently reducing variability in quality characteristics are two key objectives of the SPC. The V_{SQR} chart is one of the visual tools for achieving these objectives. The motivation of this article is to suggest an enhanced monitoring scheme for the V_{SQR} chart for monitoring the scale factor of the Rayleigh model under EWMA framework.

The following sections will be covered in the rest of the paper. Section II covers the preliminaries, Section III presents the suggested control chart and other important aspects of the proposed model, Section IV outlines the performance characteristics of the suggested design, Section V explains how to generate simulated data and implement the proposed chart, Section VI compares the proposed chart to existing design, Section VII provides an illustrative example of the proposed design. The results and conclusions of the proposed chart are discussed in Section VIII.

II. BASIC RESULTS

This section provides an overview of the Rayleigh distribution and introduces it in a cohesive context. The following concepts link the familiarization of the underlying Rayleigh data-generated process and its applications in the process monitoring charts.

The probability density function (PDF) and distribution function (DF) of the Rayleigh model with a single scale, parameter are respectively described as:

$$f_{(z,\varphi)} = \frac{1}{\varphi^2} e^{-\frac{1}{2}\left(\frac{1}{\varphi}\right)^2}; z \geq 0, \varphi > 0 \tag{1}$$

$$F(z,\varphi) = 1 - e^{-\frac{1}{2}\left(\frac{1}{\varphi}\right)^2}; z \geq 0, \varphi > 0 \tag{2}$$

where z are realizations of the Rayleigh followed random variable Z, and φ is the scale parameter. In the framework of probability theory, PDF and DF are defined as the integral of the variable density over a specified range. The PDF function whose general integral from any two points z_1 to z_2 equals the likelihood that the variate will fall within that range. Whereas, the likelihood that the variate assumes a value less than or equal to point z is expressed as $H(z, \varphi)$. The parameter φ denotes simply the scale factor whose different values result in various density curves of the Rayleigh distribution. The graphs of PDF and DF for a continuous Rayleigh random variable with different values of the scale parameter are respectively given in Figure 1.

Figure 1(a) illustrates that the densities are asymmetric and skewed toward the right, particularly for smaller values of φ. Although the graph varies with different values of φ, the Rayleigh skewness parameter remains constant. In addition, Figure 1(b) depicts the overall behavior of DF, which is right continuous, steadily increases, and varies in the interval [0, 1].

Most studies employ the traditional maximum likelihood (ML) approach to estimate the Rayleigh distribution's parameter. Consider a set of m observations $z_1, z_2, \ldots, z_m$ are taken as a random sample from the Rayleigh model. The point estimator based on the ML approach is given by:

$$\hat{\varphi} = \sqrt{\frac{\sum_{i=1}^{m} z_i^2}{2m}} \tag{3}$$

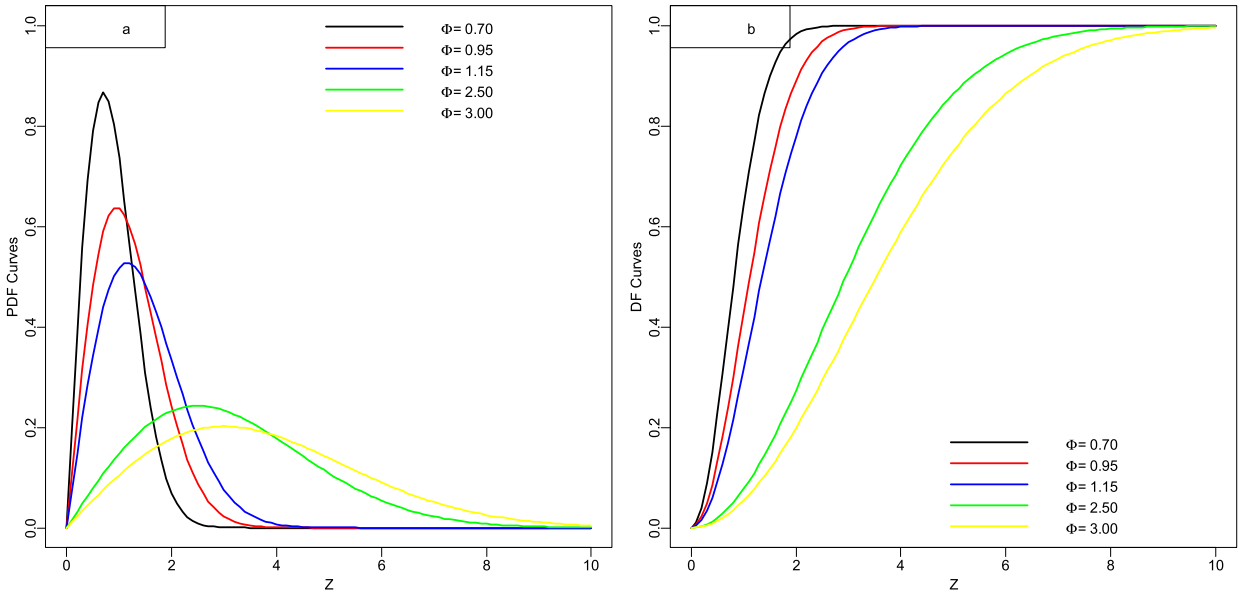

FIGURE 1. Graphs of the Rayleigh distribution at various values of the scale parameter (a) PDF (b) DF.

Now the derivation of V_R-control chart is established on the distribution of the following defined random variable.

$$V_R = \frac{\sum_{i=1}^{m} z_i^2}{2m} \tag{4}$$

where the random variable Z_i follows the Rayleigh distribution and definition corresponds to the underlying fixed realization

$$\hat{\varphi}^2 = \frac{\sum_{i=1}^{m} z_i^2}{2m} \tag{5}$$

The prime distribution of V_R is a gamma distribution with parameters m and $\frac{\varphi^2}{m}$, so the V_R-control design having the following parameters:

$$\left.\begin{aligned} LCL &= E\,(V_R) - T * SD(V_R) \\ UCL &= E(V_R) + T * SD(V_R) \end{aligned}\right\} \tag{6}$$

where the T is a quantile of the gamma distribution for a constant value of type-I error, and V_R is an unbiased estimator of φ^2.

The control chart design is based on a positive skewed square root design of V_{SQR}-statistic is given by:

$$V_{SQR} = \sqrt{\frac{\sum_{i=1}^{m} Z_i^2}{2m}} \tag{7}$$

where $\sqrt{\sum_{i=1}^{m} Z_i^2}$ follows the chi model with a degree of freedom 2m [23].

Thus the PDF ofrandom variable R can be expressed as:

$$f_{(r,n)} = \frac{2^{1-m} r^{2m-1} e^{-\frac{r^2}{2}}}{\sqrt{m}} \tag{8}$$

Statistical average and variance of the random variable R can be expressed as:

$$\left.\begin{aligned} E\,(R) &= \frac{\sqrt{2}\Gamma(m+\frac{1}{2})}{\Gamma m} \\ Var\,(R) &= 2(m - (\frac{\Gamma(\left(m+\frac{1}{2}\right))^2}{\Gamma m}) \end{aligned}\right\} \tag{9}$$

Estimate the average and scale parameters of the random variable V_{SQR}.

Then the average and variance of the desired statistic V_{SQR}, utilizing the pivotal quantity can be established as [19]:

$$\left.\begin{aligned} E\left(V_{SQR}\right) &= \varphi A_{(m)} \\ Var\left(V_{SQR}\right) &= \varphi^2[1-A_{(m)^2}] \end{aligned}\right\} \tag{10}$$

The T-sigma limits of V_{SQR}-chart based on the corresponding sampling distribution of square root statistic are established as given below:

$$\left.\begin{aligned} LCL &= \varphi A_{(m)} - T\varphi\sqrt{1 - A_{(m)}^2} \\ UCL &= \varphi A_{(m)} + T\varphi\sqrt{1 - A_{(m)}^2} \end{aligned}\right\} \tag{11}$$

where $A_{(m)} = \frac{\Gamma(m+\frac{1}{2})}{\sqrt{m}\Gamma m}$ is sample size dependent function, and T is the quantile of the chi distribution, chosen according to the set the value of false alarm rate α.

Both designs are commonly used for monitoring the scale parameter of Rayleigh distributed processes. However, the efficiency performance in terms of average run length (ARL) and power curves indicates that V_{SQR}-chart is better performance in identifying the moderate to larger changes in the scaling factor φ. To further enhance the out-control performance of V_{SQR}-chart in conditions of smaller to moderate shifts in the studied parameter. The REWMA charting procedure is outlined in the following section.

III. PROPOSED CHART

The procedure of the proposed REWMA chart has been described in this section. Let the under-study quality characteristic assumes the Rayleigh distribution as given in Eq. (1). Suppose the realizations $z_1, z_2, \ldots z_n$ constitute a random sample of size n from the Rayleigh model with scale parameter φ. The geometric moving average (GMA) scheme based on the statistic of interest can be defined as follows:

$$Y_i = (1-\pi)\, Y_{i-1} + \pi V_{SQRi} \tag{12}$$

where Y_i is a realization of the GMA at time i(i = 0, 1 ....) and smoothing quantity π belongs to an interval limit zero and one, i.e., $\pi \in]0, 1]$. The sequentially recorded observations V_{SQRi} are the estimated values calculated for each subgroup of size n over the designed sampling scheme. The smoothing weights π decease exponentially as in the geometric expansion. The initial value Y_0 is often set as to be the monitoring quantity. Due to the resembling Eq. (12) to geometric progression, many other properties of GMA can be established.

The realizations Y_i in Eq. (12) can be alternatively expressed in terms of the moving average of past and current observations as follows:

$$\left.\begin{aligned} Y_0 &= \varphi_0, \\ Y_i &= (1-\pi)^i\, Y_0 + \textstyle\sum_{j=0}^{i-1} \pi\,(1-\pi)^j\, V_{SQ(i-j)} \end{aligned}\right\} \tag{13}$$

where the initial value set to the target value and the weighting quantity $\pi\,(1-\pi)^j$ fall off in an exponential pattern as observations turn into less recent status.

Because of the smoothing process, the influence of a value on the test statistic decreases exponentially with time or with the number of additional observations, with the weighting factor controlling the decay rate. The proposed REWMA chart is more flexible design because setting the smoothing constant π equal to 1 yields the conventional V_{SQR}-chart. In this way, the suggested REWMA process monitoring scheme represents a generalized structure of the Shewhart-type V_{SQR}-chart. Thus the parameters of the proposed REWMA are the statistic Y_i, lower control limit (LCL) and upper control limit (UCL) as given below:

$$\left.\begin{aligned} UCL &= \varphi A_{(m)} + TS_{(V_{SQR})}\sqrt{(\tfrac{\pi}{2-\pi})[1-(1-\pi)^{2i}]} \\ LCL &= \varphi A_{(m)} - TS_{(V_{SQR})}\sqrt{(\tfrac{\pi}{2-\pi})[1-(1-\pi)^{2i}]} \end{aligned}\right\} \tag{14}$$

where $E(V_{SQR}) = \varphi A_{(m)}$ and $S_{(V_{SQR})} = \varphi\sqrt{1-A^2_{(m)}}$ respectively mean and standard deviation of the V_{SQR} estimator, and T is the adjustment factor used for the symmetrical construction of the proposed chart. The value of l is usually adjustable by thefalse alarm rate.

Alternatively Eq. (14) can be rewritten as:

$$\left.\begin{aligned} LCL &= \varphi G_1 \\ UCL &= \varphi G_2 \end{aligned}\right\} \tag{15}$$

where $Q_1 = A_{(m)} - TS_{(V_{SQR})}\sqrt{(\frac{\pi}{2-\pi})[1-(1-\pi)^{2i}]}$ and $Q_2 = A_{(m)} + TS_{(V_{SQR})}\sqrt{(\frac{\pi}{2-\pi})[1-(1-\pi)^{2i}]}$

Whenever Y_i lies behind the control limits LCL and UCL, the process is assumed to be in the state of instability, and action should be taken with the intention of swiftly identifying uncontrollable situations.

Limits given in Eq. (15) are time varying i.e., changes with time period i.

As i becomes large, the quantity $[1-(1-\pi)^{2i}]$ approaches to unity. Thus the steady form of control limits in case of a larger value of i can be written as:

$$\left.\begin{aligned} UCL &= \varphi A_{(m)} + TS_{(V_{SQR})}\sqrt{\tfrac{\pi}{2-\pi}} \\ LCL &= \varphi A_{(m)} - TS_{(V_{SQR})}\sqrt{\tfrac{\pi}{2-\pi}} \end{aligned}\right\} \tag{16}$$

However, the exact limits given in Eq. (15) are strongly recommended for the construction of the proposed chart. Exact limits improve the control chart's ability to indentify an off-target state quickly after the REWMA scheme is initiated. Usage of proposed described above based on the assumption that in-control state parameter is know. However process parameters are typically not available in certain situations and are approximated using an in-control retrospective.

In the case of an estimated value of φ, Eq. (15) can be written as:

$$\left.\begin{aligned} LCL &= \bar{\hat{\varphi}} G_1 \\ UCL &= \bar{\hat{\varphi}} G_2 \end{aligned}\right\} \tag{17}$$

where $\bar{\hat{\varphi}} = \frac{\sum_{j=1}^{K} \hat{V}_{SQRj}}{K}$ and K are available preliminary samples. The adjustment factor T can be obtained using the Monte Carlo simulation. To perform the Monte Carlo simulation scale factor φ is set to be 1.5 and data is generated from the sampling distribution of V_{SQR} statistic. Simulation runs are performed until we get the pre-specified value of in-control ARL. In our case and in-control ARL of 100 is used and value of T are computed across the different sample sizes. Thus the values of T that determine the width of the proposed chart and subsequently utilize in obtaining the factors G_1 and G_2 are provided in Table 1.

Table 1 shows the values of factor T computed from the Monte Carlo experiment of 10^5 runs such that pre-specified value of in-control ARL is approximately obtained. Additionally, the values of factors G_1 and G_2 are computed and given in Tables 2-4 for different values of smoothing constant and sample sizes.

Tables 2-4 show values for the coefficients G_1 and G_2 that can ease the computation work of the proposed chart, and control limits can be constructed without involving the adjustment factor l.

IV. PERFORMANCE MEASURES

In this section, the RL distribution properties are presented to assess the statistical performance of the proposed chart. An extensive simulation is performed to evaluate the performance of the REWMA chart. Let us assume by

TABLE 1. Computed values of the factor T for REWMA chart.

Sample	In control average run length value equal to 100				
	π=0.04	π=0.08	π=0.20	π=0.40	π=0.60
			T		
2	2.988	2.336	2.396	2.494	2.548
3	2.618	2.270	2.388	2.494	2.536
4	2.465	2.233	2.378	2.499	2.546
5	2.352	2.216	2.383	2.502	2.547
6	2.281	2.200	2.384	2.498	2.543
8	2.198	2.157	2.384	2.505	2.549
10	2.140	2.173	2.382	2.506	2.555
12	2.096	2.149	2.366	2.499	2.549

TABLE 2. Coefficients $= G_1$ and G_2 for the proposed scheme at $\pi = 0.04$.

Time index	Sample size					
	3		5		10	
	G_1	G_2	G_1	G_2	G_1	G_2
1	0.9298	0.9889	0.9546	0.9961	0.9741	1.0010
2	0.9184	1.0003	0.9466	1.0041	0.9689	1.0062
3	0.9102	1.0086	0.9408	1.0099	0.9652	1.0100
4	0.9037	1.0151	0.9362	1.0145	0.9622	1.0129
5	0.8983	1.0205	0.9324	1.0183	0.9598	1.0154
6	0.8937	1.0250	0.9292	1.0215	0.9577	1.0175
8	0.8863	1.0324	0.9240	1.0267	0.9543	1.0208
10	0.8805	1.0382	0.9200	1.0307	0.9517	1.0235
12	0.8760	1.0428	0.9168	1.0339	0.9496	1.0255
14	0.8723	1.0465	0.9142	1.0365	0.9479	1.0272
16	0.8693	1.0495	0.9120	1.0387	0.9466	1.0286
18	0.8668	1.0520	0.9103	1.0404	0.9454	1.0297

TABLE 3. Coefficients G_1 and G_2 for the proposed scheme at $\pi = 0.20$.

Time index	Sample size					
	3		5		10	
	G_1	G_2	G_1	G_2	G_1	G_2
1	0.8246	1.0941	0.8702	1.0805	0.9127	1.0624
2	0.7868	1.1319	0.8407	1.1100	0.8917	1.0834
3	0.7664	1.1523	0.8248	1.1259	0.8804	1.0947
4	0.7545	1.1643	0.8154	1.1353	0.8738	1.1014
5	0.7472	1.1716	0.8097	1.1410	0.8697	1.1054
6	0.7426	1.1761	0.8062	1.1445	0.8672	1.1080
8	0.7380	1.1808	0.8026	1.1481	0.8646	1.1106
10	0.7361	1.1827	0.8011	1.1496	0.8636	1.1116
12	0.7353	1.1834	0.8005	1.1502	0.8631	1.1120
14	0.7350	1.1837	0.8002	1.1505	0.8630	1.1122
16	0.7349	1.1839	0.8001	1.1506	0.8629	1.1123
18	0.7348	1.1839	0.8001	1.1506	0.8629	1.1123

discussing the scenario where the production process is in the state of IC. The REWMA chart could give false signals of process distributional shifts because the control limits are used as decision-making thresholds, and observed data are random. In terms of testing a hypothesis, this is called the type-I error. Thus in the context of hypothesis, we have to observe if the process changes its in-control state or not. We formulate our problem by adopting the following hypothesis:

H_0: $\varphi = \varphi_0$; i.e., process is in-control at the target state φ_0

H_1: $\varphi = \Delta\varphi_0 = \varphi_1$; i.e., process is shifted to another state φ_1.

The RL is a collection of samples from the initial time of consideration until the process triggers an OC signal. The

TABLE 4. Coefficients G_1 and G_2 for the proposed scheme at $\pi = 0.60$.

Time index	Sample size					
	3		5		10	
	G_1	G_2	G_1	G_2	G_1	G_2
1	0.5300	1.3887	0.6381	1.3126	0.7468	1.2284
2	0.4970	1.4218	0.6122	1.3385	0.7282	1.2470
3	0.4919	1.4268	0.6082	1.3425	0.7254	1.2498
4	0.4911	1.4276	0.6075	1.3432	0.7249	1.2503
5	0.4910	1.4278	0.6074	1.3433	0.7248	1.2503
6	0.4909	1.4278	0.6074	1.3433	0.7248	1.2504
8	0.4909	1.4278	0.6074	1.3433	0.7248	1.2504
10	0.4909	1.4278	0.6074	1.3433	0.7248	1.2504
12	0.4909	1.4278	0.6074	1.3433	0.7248	1.2504
14	0.4909	1.4278	0.6074	1.3433	0.7248	1.2504
16	0.4909	1.4278	0.6074	1.3433	0.7248	1.2504
18	0.4909	1.4278	0.6074	1.3433	0.7248	1.2504

TABLE 5. Performance of the REWMA chart at the set value $ARL_0 = 100$.

Shifting parameter	$\pi = 0.04$								
	$n = 2$			$n = 5$			$n = 8$		
	ARL	MRL	SDRL	ARL	MRL	SDRL	ARL	MRL	SDRL
1.00	99.64	68.72	99.14	99.89	68.89	99.39	99.97	68.95	99.47
1.04	29.23	19.91	28.73	23.04	15.62	22.53	19.13	12.91	18.62
1.06	14.22	9.51	13.71	12.23	8.13	11.72	9.96	6.55	9.45
1.08	7.75	5.02	7.23	7.38	4.76	6.86	6.06	3.84	5.54
1.12	3.76	2.24	3.22	3.79	2.26	3.25	3.18	1.84	2.63
1.15	2.76	1.54	2.2	2.7	1.5	2.14	2.24	1.17	1.67
1.18	2.04	1.03	1.46	2.09	1.06	1.51	1.8	0.85	1.2
1.20	1.86	0.9	1.26	1.85	0.89	1.25	1.62	0.72	1
1.50	1.08	0.27	0.29	1.06	0.24	0.25	1.04	0.21	0.2
1.80	1.02	0.18	0.14	1.01	0.15	0.1	1	0	0
2.00	1.01	0.15	0.10	1	0	0	1	0	0

RL is obviously a random variable because it is determined by the observed random samples, which are assumed to be independent and collected over equally space-time point. The average of the RL is usually denoted by ARL which can be estimated both for IC state (ARL_0) and OC state (ARL_1) of the underlying process. The ideal circumstance for a particular control chart is, of course, its ARL_1 value to be small and its ARL_0 value to be large, but this is difficult to attain. In the control charts theory, we often fix the ARL_0 value at a certain level and work to make the ARL_1 number as less as feasible to find a compromised value. The computation of ARL value is estimated via Monte Carlo simulation using the following formula:

$$\mathrm{ARL} = \frac{\sum_{i=1}^{M} \mathrm{RL_i}}{M} \tag{18}$$

where RL_i is run length at ith run and M is the number of total simulated runs. The usage of ARL as a performance metric may not be adequate due to the large standard deviation (i.e., high skewness) of RL distribution in the case of Rayleigh distribution.Due to the possibility of inaccurate interpretations based on the ARL measure, we have additionally considered the standard deviation and median of the RL distribution as performance metrics. The skewness of run RL distribution has a lesser impact on the median run length (MRL) and it is still the 50th percentile of the RL distribution. In simulation procedure, we have computed the values of performance metrics under different IC and OC scenarios of the Rayleigh process by assuming the IC scale parameter value equal to 1.5. Computed values of ARL at a fixed value of smoothing constant are shown in Tables 5-6.

Table 5 provides the overall behavior of the REWMA chart in terms of performance metrics under a substantial range of increases in the scale parameter values. It can observe that the ARL forthe IC state process is relatively closer to the set value of ARL_0 across the different sample sizes. Whereas ARL for OC state continuously decreases as with an increase in φ. For instance, ARL values to detect a shift of 8% increase in scaling parameter are approximately reduced to (35, 23 and 18) for sample sizes (2, 5, and 8) respectively. Whereas the MRL values for the same increase are approximately reduced (24, 16 and 12) for sample sizes (2, 5, and 8), respectively. The same discussion holds for results presented in Table 6, and

TABLE 6. Performance of the REWMA chart at the set value $ARL_0 = 100$.

Shifting parameter	Smoothing constant $\pi = 0.20$								
	$n = 2$			$n = 5$			$n = 8$		
	ARL	MRL	SDRL	ARL	MRL	SDRL	ARL	MRL	SDRL
1.00	100.23	69.13	99.73	100.14	69.06	99.64	99.64	68.72	99.14
1.04	61.29	42.14	60.79	50.32	34.53	49.82	42.62	29.19	42.12
1.06	46.83	32.11	46.33	33.48	22.86	32.98	26.79	18.22	26.29
1.08	35.83	24.49	35.33	23.78	16.13	23.27	18.2	12.27	17.69
1.12	22.37	15.16	21.86	13.36	8.91	12.85	9.6	6.3	9.09
1.15	16.48	11.07	15.97	9.44	6.19	8.93	6.74	4.32	6.22
1.18	12.78	8.51	12.27	7.17	4.61	6.65	5.09	3.17	4.56
1.20	11	7.27	10.49	6.1	3.87	5.58	4.34	2.65	3.81
1.50	2.96	1.68	2.41	1.81	0.86	1.21	1.42	0.57	0.77
1.80	1.82	0.87	1.22	1.25	0.43	0.56	1.09	0.28	0.31
2.00	1.51	0.64	0.88	1.12	0.31	0.37	1.03	0.2	0.18

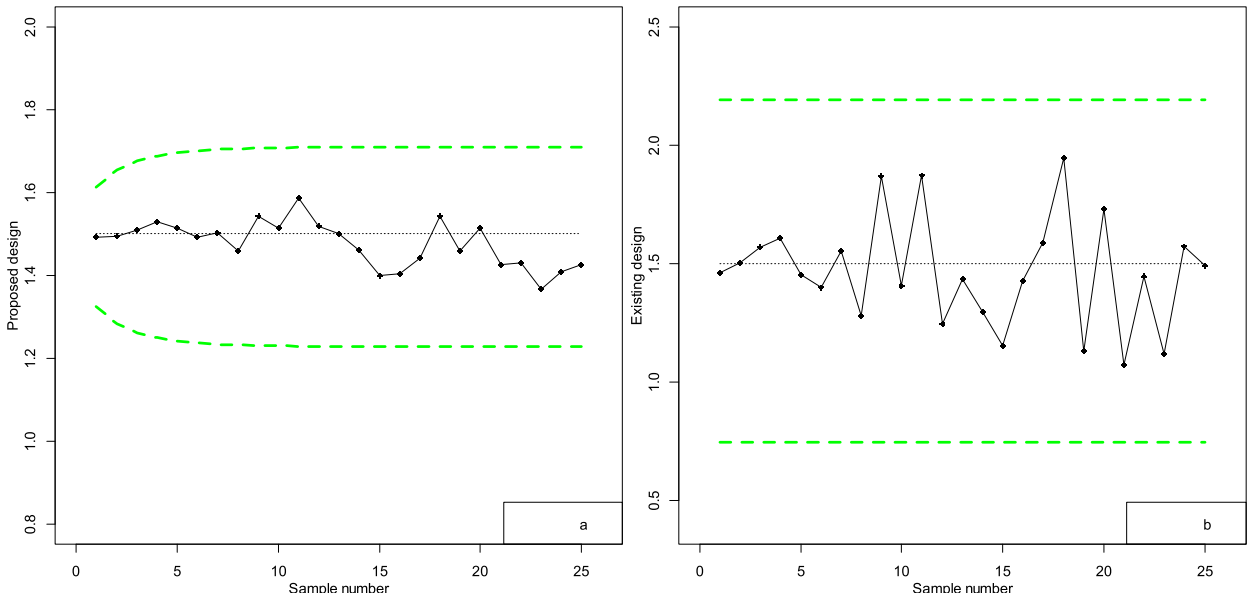

FIGURE 2. The REWMA chart and V_{SQR} chart for IC process.

measuring indicators exhibit similar types of behavior under different incremental shifts in the scale parameter values.

V. SIMULATION ANALYSES

In this section, the theory of the REWMA chart and its effectiveness for detecting the smaller incremental changes in target parameter are easily demonstrated using simulated data. The simulated data is considered to validate the performance of the REWMA chart for detecting the smaller shifts. To do so, a random sample of 25 observations are randomly generated from the Rayleigh distribution with scale parameter $\varphi = 1.5$ using the ShotGroups package in R software. These 25 observations are plotted in Figure 2 on the conventional Shewhart type V_{SQR} chart with set-up values $ARL_0 = 100$ and $n = 5$ and the proposed chart with $ARL_0 = 100$, $n = 6$ and $\Delta = 0.20$.

Note that all plotted points in Figure 2 are within the designated limits, indicating that the underlying process is in a state of statistical control. Now to validate the sensitivity of proposed control chart for detecting shift, another random sample of 10 values is selected from the Rayleigh distribution with scale parameter values $\varphi = (0.90, 0.94)$ which are 18% and 28% increased, respectively in the target value.These 10 observations may be considered a sample from an OC state phase of the process after the process has exhibited a shift in the observed parameter φ of amounts 20% and 30%, respectively. Consequently, the process can assume to be in an OC state, and the last 10 values are also plotted in Figure 3 and Figure 4

Figure 3(a) shows that there is a convincing indication that the process is OC state because after 15^{th} points, all points have upward drift and are above the central line, whereas the traditional V_{SQ} chart in Figure 3(b) is still indicating the IC status of the process and is unable to detect a shift of smaller amount in the study parameter. Likewise, in Figure 4, the REWMA effectively detects the abrupt change in the

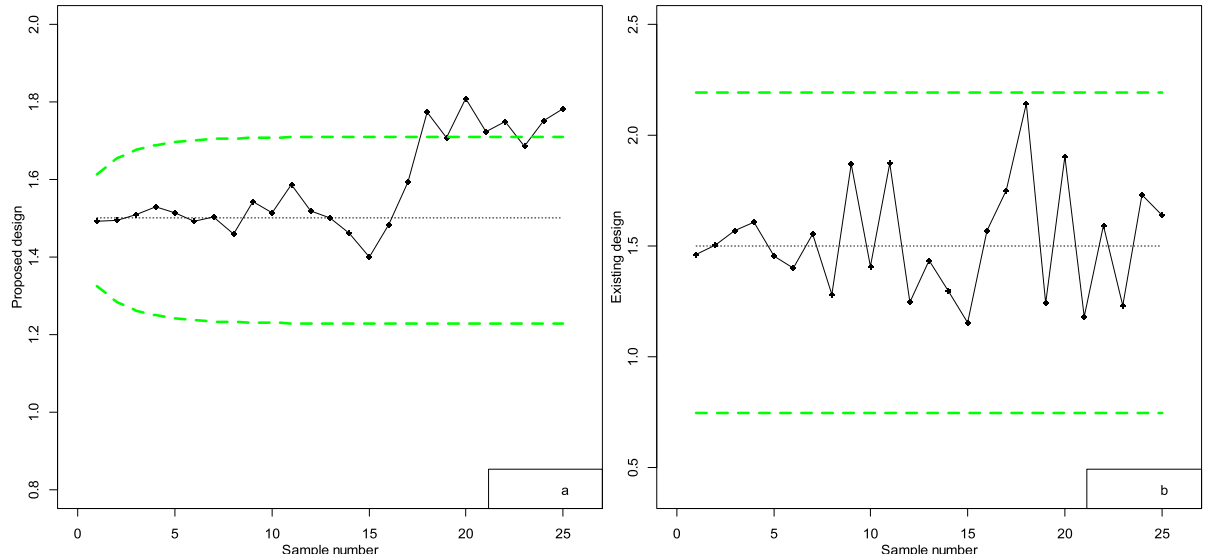

FIGURE 3. The REWMA chart and V_{SQR} chart with 18% increment in the monitoring target.

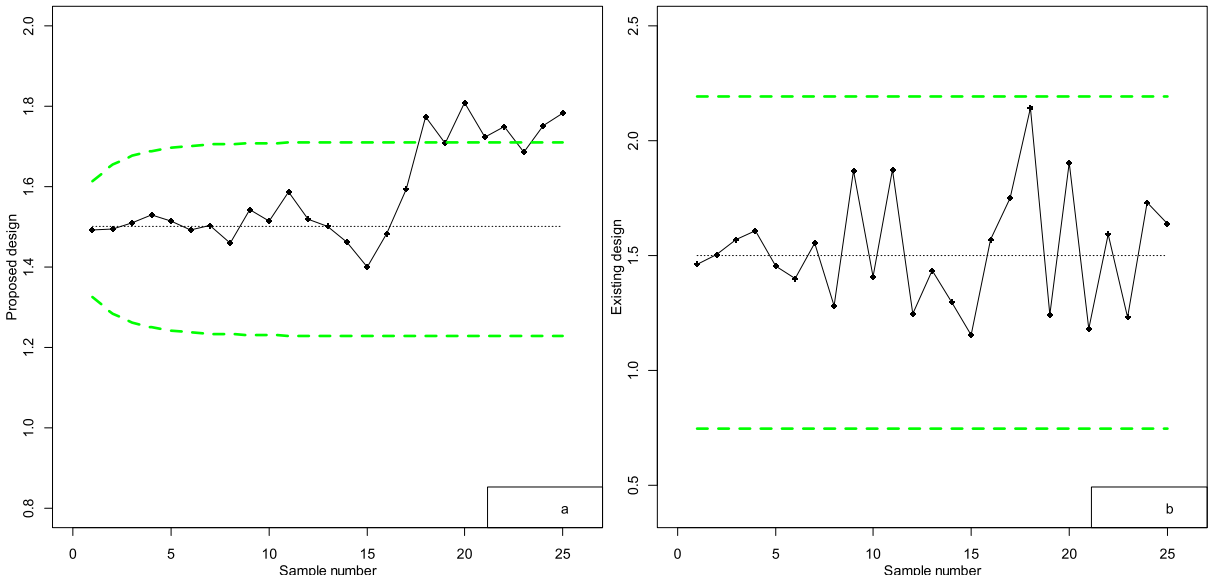

FIGURE 4. The REWMA chart and V_{SQR} chart with 28% increment in the monitoring target.

target parameter. On the contrary; V_{SQR} chart does not provide stronger evidence of the OC state of the process, which is in fact OC after the 15th sample. Of course, the relatively minor size of the change in the target parameter is to account for this failure.

VI. COMPARISON STUDY

We compare our suggested chart in this section to its counterpart for the Rayleigh quality characteristic in terms of power curves. In the control chart framework, it indicates the likelihood of rejecting a lot of substandard quality or allowing a process to continue in operation if it is performing satisfactorily in relation to some quality feature. Therefore, the likelihood of correctly rejecting the null hypothesis that the process is in an IC state is represented by the term ''power.''Statistically, the term power means one minus the probability of type-II error. Generally, the value of type-II error is based on sample size, and a smaller value of this error is expected at a larger sample size. Now in our case, we use power curves as efficiency metric to compare and contrast the REWMA and V_{SQR} charts. Using the designed limits given in (14) and (16) power curves of the REWMA chart and V_{SQR} chart have been computed at different values of n and $ARL_0 = 100$. Power curves of the proposed chart have been evaluated at smoothing constant $\pi = 0.40$, and results obtained in comparison with V_{SQR} chart are shown in Figure 5.

Power curves plotted in Figure 5 indicate that both charts perform similarly when the constant shift value equal to one, i.e., the underlying process is in an IC state. At IC state,

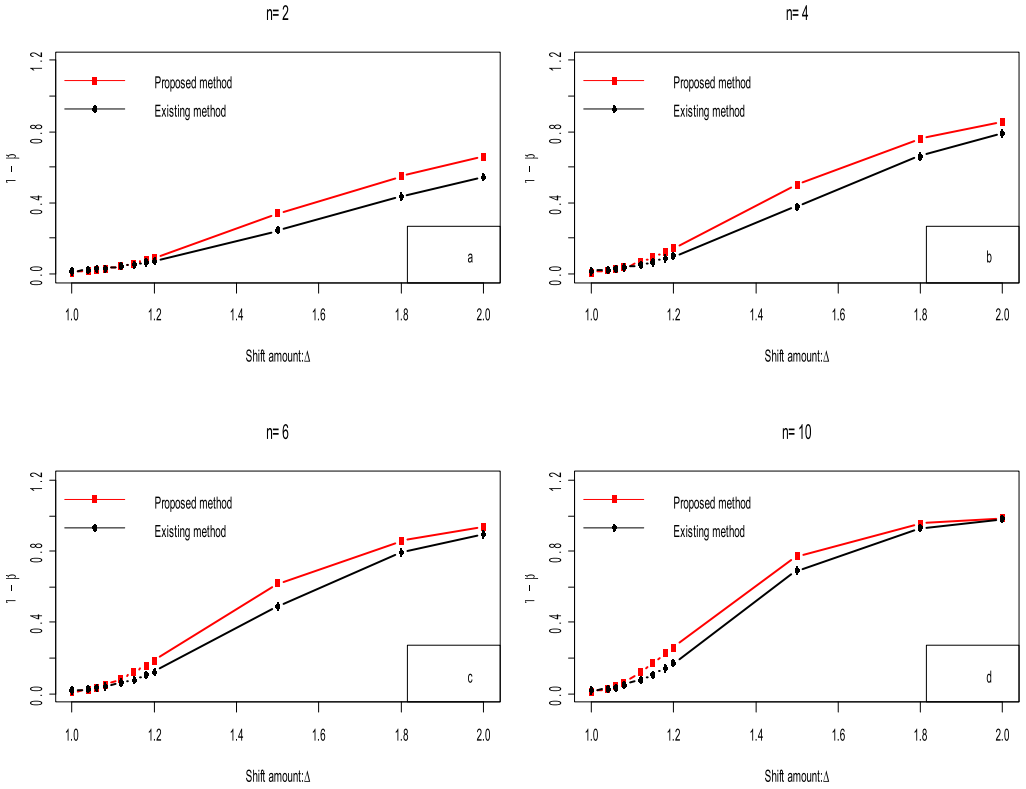

FIGURE 5. Computed power comparisons of the suggested chart and V_{SQR} chart.

both charts provide power closer to presume the value of α, i.e., 0.01, and it yields $ARL_0 = 100$. As the process departs from the prescribed target, both control charts result in raising in power. However, the proposed REMWA chart performs efficiently to detect any abrupt increase in the scale parameter value of the Rayleigh process as compared to the V_{SQR} chart. For instance, the associated power of the proposed chart for detecting the shift of amount (10%, 20% and 30%) increases in φ at $n = 5$ are approximately (0.019, 0.063, and 0.132), which are higher than the corresponding powers of the V_{SQR} chart, i.e., (0.003, 0.004 and 0.006).

The same holds for other sample sizes and overall, the power of both charts increases with an increase in sample size. The V_{SQR} chart performs equivalently to the proposed chart for detecting a considerably larger shift size. In general, Figure 5 suggests that the proposed chart is quicker and more effective for detecting smaller increases in the scale factor of the Rayleigh quality characteristic.

VII. DATA APPLICATION

We demonstrate the usefulness of the REWMA control chart using a real-life dataset, which contains the breakdown times of 25 ball bearings during the survival test as reported by Caroni [31]. This dataset is commonly used in survival analysis to show the applications of statistical models for predicting lifetime [32], [33]. Our goal is not to compare various models for this particular dataset, but rather to explain how the REWMA method can be applied to real-life data. To evaluate the accuracy of the Rayleigh distribution, we use subjective probability plots. These plots are a useful tool for identifying the probability distribution that is most suitable for modeling the data.

TABLE 7. Data on bearing failure times.

Sample Number	Observations			
	First	Second	Third	$\hat{V}_{SQR}$
1	17.88	28.92	33.00	19.34
2	93.12	98.64	105.12	70.06
3	48.48	51.84	51.96	35.91
4	41.52	42.12	45.60	30.49
5	67.80	67.80	68.64	48.14
6	105.84	127.92	128.0	85.59
7	54.12	555.56	67.80	42.05
8	86.64	68.88	84.12	83.32

Figure 6 presents the fitting plots of the Rayleigh model applied to the dataset. Subjective evaluation of the plots suggests that the dataset follows the Rayleigh distribution more reasonably. Formal statistical tests, such as the Kolmogorov–Smirnov (KS) test, can also be used to confirm the appropriateness of the model. The results of the KS test for the fatigue failure time dataset show a distance of 0.209 and a p-value of 0.620, indicating that the Rayleigh distribution is a suitable model for the data. Therefore, we can use the dataset to build our proposed control chart. We divide the data into subgroups of size 3, resulting in a total of 8 subgroups, which we then use to construct the chart. The bearing failure times in millions of revolutions are as follows:

The estimated value of $\hat{V}_{SQR}$ for each subgroup has been calculated using equation (5) and is provided in the last

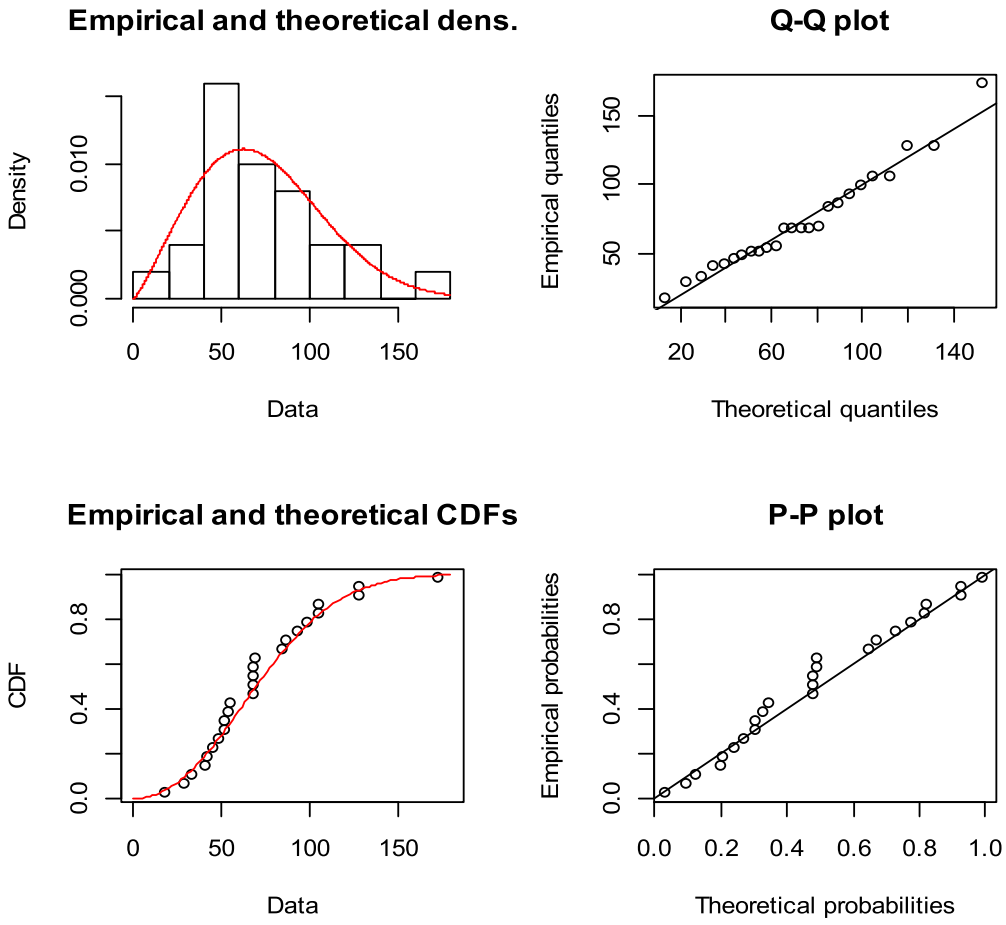

FIGURE 6. Basic fitting plots of the Rayleigh distribution.

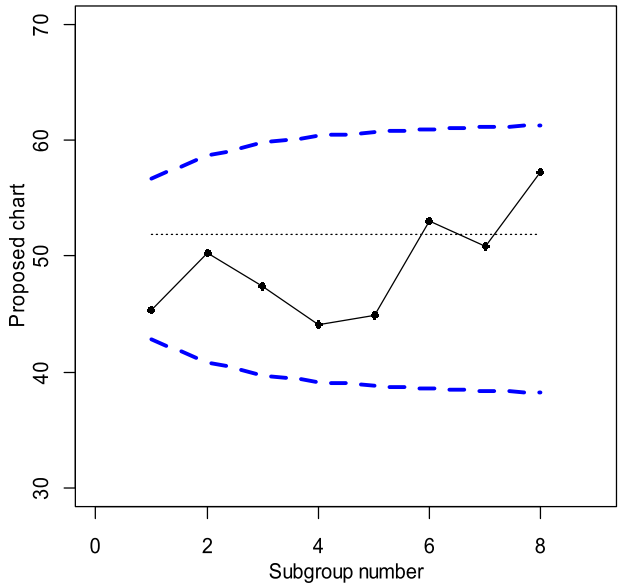

FIGURE 7. Proposed control chart for failure times of ball bearing data.

column of Table 7. Based on the proposed design of the REWMA chart for the ball bearing data, the maximum likelihood estimate of φ is 48.544. To construct time-varying control limits, we use the G_1 and G_2 coefficients for $n = 3$ as listed in Table 3. Figure 7 shows a graphical display of the REWMA chart based on these values. Figure 7 reveals that all of the data points are within the control limits, which indicates that the Rayleigh scale parameter is within the expected range and there are no abnormal patterns present. The data points are observed to be concentrated around the center line, indicating that the data generating process is operating within expected limits.

VIII. CONCLUSION

In this work, a new monitoring scheme, namely the REWMA chart for observing the scaling parameter of the Rayleigh distributed process, has been devised. The proposed chart has been designated on the sampling distribution of the ML estimator of the Rayleigh quality characteristic under the framework of the EWMA chart. Some formulae and designated limits are derived to aid the practical implementation of the suggested chart. The proposed design is the best alternative of the V_{SQR} chart in terms of detecting smaller shifts in the target parameter. The proposed REWMA chart design parameters have been computed for various sample sizes under the assumption of Rayleigh output data. The essential statistical features such as ARL, MRL, and SDRL of the suggested

chart are evaluated through the Monte Carlo experiment. Numerical findings based on performance evaluation reveal that the suggested chart outperforms at reasonably larger sample sizes. Simulation analysis also indicates the considerable improvement of the REWMA chart over the existing procedure in detecting shifts of smaller sizes in the study parameter. The proposed scheme has been compared with its counterpart in terms of the power function. The comparative evaluation leads to suggest that the REWMA chart is quicker and highly efficient for the smaller to moderate increments in the scale factor of the Rayleigh characteristic.

In addition, a real data example has been considered to describe the computation procedure of the REWMA chart.

Acknowledgment

The authors extend their appreciation to Prince Sattam Bin Abdulaziz University for funding this research work through the project number (PSAU/2022/01/21867)

REFERENCES

[1] K. Bisiotis, S. Psarakis, and A. N. Yannacopoulos, "Control charts in financial applications: An overview," *Qual. Rel. Eng. Int.*, vol. 38, no. 3, pp. 1441–1462, Apr. 2022.
[2] A. R. Abbasi and M. R. Mahmoudi, "Application of statistical control charts to discriminate transformer winding defects," *Electr. Power Syst. Res.*, vol. 191, Feb. 2021, Art. no. 106890.
[3] C. Park, L. Ouyang, and M. Wang, "Robust g-type quality control charts for monitoring nonconformities," *Comput. Ind. Eng.*, vol. 162, Dec. 2021, Art. no. 107765.
[4] S. Kinat, M. Amin, and T. Mahmood, "GLM-based control charts for the inverse Gaussian distributed response variable," *Qual. Rel. Eng. Int.*, vol. 36, no. 2, pp. 765–783, Mar. 2020.
[5] K. Park, D. Jung, and J. Kim, "Control charts based on randomized quantile residuals," *Appl. Stochastic Models Bus. Ind.*, vol. 36, no. 4, pp. 716–729, Jul. 2020.
[6] L. Lee Ho, F. H. Fernandes, and M. Bourguignon, "Control charts to monitor rates and proportions," *Qual. Rel. Eng. Int.*, vol. 35, no. 1, pp. 74–83, Feb. 2019.
[7] F. Shah, Z. Khan, M. Aslam, and S. Kadry, "Statistical development of the V_{SQ}-control chart for extreme data with an application to the carbon fiber industry," *Math. Problems Eng.*, vol. 2021, pp. 1–11, Jul. 2021.
[8] N. Saengsura, S. Sukparungsee, and Y. Areepong, "Mixed moving average-cumulative sum control chart for monitoring parameter change," *Intell. Autom. Soft Comput.*, vol. 31, no. 1, pp. 635–647, 2022.
[9] J. O. Ajadi, Z. Wang, and I. M. Zwetsloot, "A review of dispersion control charts for multivariate individual observations," *Qual. Eng.*, vol. 33, no. 1, pp. 60–75, Jan. 2021.
[10] İ. Kaya, M. Erdoğan, and C. Yıldız, "Analysis and control of variability by using fuzzy individual control charts," *Appl. Soft Comput.*, vol. 51, pp. 370–381, Feb. 2017.
[11] W. A. Shewhart, "Quality control charts," *Bell Syst. Tech. J.*, vol. 5, no. 4, pp. 593–603, 1926.
[12] S. Ali, A. Pievatolo, and R. Göb, "An overview of control charts for high-quality processes," *Qual. Rel. Eng. Int.*, vol. 32, no. 7, pp. 2171–2189, Nov. 2016.
[13] S. A. Abbasi, M. Riaz, A. Miller, S. Ahmad, and H. Z. Nazir, "EWMA dispersion control charts for normal and non-normal processes," *Qual. Rel. Eng. Int.*, vol. 31, no. 8, pp. 1691–1704, Dec. 2015.
[14] B. John and S. M. Subhani, "A modified control chart for monitoring non-normal characteristics," *Int. J. Product. Qual. Manag.*, vol. 29, no. 3, pp. 309–328, May 2020.
[15] Z. Khan, M. Gulistan, W. Chammam, S. Kadry, and Y. Nam, "A new dispersion control chart for handling the neutrosophic data," *IEEE Access*, vol. 8, pp. 96006–96015, 2020.
[16] Z. Khan, M. Gulistan, N. Kausar, and C. Park, "Neutrosophic Rayleigh model with some basic characteristics and engineering applications," *IEEE Access*, vol. 9, pp. 71277–71283, 2021.
[17] D. Karagöz and C. Hamurkaroğlu, "Control charts for skewed distributions," *Adv. Methodol. Statist.*, vol. 9, no. 2, pp. 95–106, Jul. 2012.
[18] E. Santiago and J. Smith, "Control charts based on the exponential distribution: Adapting runs rules for the *t* chart," *Qual. Eng.*, vol. 25, no. 2, pp. 85–96, Apr. 2013.
[19] K. Rosaiah, B. S. Rao, J. P. Reddy, and C. Chinnamamba, "Variable control charts for Gumbel distribution based on percentiles," *J. Comput. Math. Sci.*, vol. 9, no. 12, pp. 1890–1897, Dec. 2018.
[20] M. P. Hossain, M. H. Omar, and M. Riaz, "New *V* control chart for the Maxwell distribution," *J. Stat. Comput. Simul.*, vol. 87, no. 3, pp. 594–606, Feb. 2017.
[21] B. Guo and B. X. Wang, "Control charts for monitoring the Weibull shape parameter based on type-II censored sample," *Qual. Rel. Eng. Int.*, vol. 30, no. 1, pp. 13–24, Feb. 2014.
[22] F.-K. Wang, B. Bizuneh, and X.-B. Cheng, "New control charts for monitoring the Weibull percentiles under complete data and type-II censoring," *Qual. Rel. Eng. Int.*, vol. 34, no. 3, pp. 403–416, Apr. 2018.
[23] Z. Khan, M. Gulistan, S. Kadry, Y. Chu, and K. Lane-Krebs, "On scale parameter monitoring of the Rayleigh distributed data using a new design," *IEEE Access*, vol. 8, pp. 188390–188400, 2020.
[24] M. P. Hossain, M. H. Omar, M. Riaz, and S. Y. Arafat, "On designing a new control chart for Rayleigh distributed processes with an application to monitor glass fiber strength," *Commun. Statist., Simul. Comput.*, vol. 51, no. 6, pp. 3168–3184, Jun. 2022.
[25] A. U. Udom, O. S. Ugwu, and T. E. Ugah, "On the results of non-normality of process characteristics on $\bar{x}$ and hotelling's X^2-control charts," *J. Statist. Manage. Syst.*, vol. 24, no. 6, pp. 1283–1300, Aug. 2021.
[26] S. Chakraborti and M. A. Graham, "Nonparametric (distribution-free) control charts: An updated overview and some results," *Qual. Eng.*, vol. 31, no. 4, pp. 523–544, Oct. 2019.
[27] C. M. Borror, D. C. Montgomery, and G. C. Runger, "Robustness of the EWMA control chart to non-normality," *J. Qual. Technol.*, vol. 31, no. 3, pp. 309–316, Jul. 1999.
[28] S. S. Alkahtani, "Robustness of DEWMA versus EWMA control charts to non-normal processes," *J. Modern Appl. Stat. Methods*, vol. 12, no. 1, pp. 148–163, May 2013.
[29] D. C. Montgomery, *Introduction to Statistical Quality Control*. New York, NY, USA: Wiley, 2019.
[30] J. Y. Liu, M. Xie, T. N. Goh, and L. Y. Chan, "A study of EWMA chart with transformed exponential data," *Int. J. Prod. Res.*, vol. 45, no. 3, pp. 743–763, Mar. 2007.
[31] C. Caroni, "The correct 'ball bearings' data," *Lifetime Data Anal.*, vol. 8, no. 4, pp. 395–399, 2002, doi: 10.1023/A:1020523006142.
[32] S. Şeker and E. Ayaz, "A reliability model for induction motor ball bearing degradation," *Electr. Mach. Power Syst.*, vol. 31, no. 7, pp. 639–652, 2010.
[33] I. K. Alsmairan and A. I. Al-Omari, "Weighted Suja distribution with application to ball bearings data," *Life Cycle Rel. Saf. Eng.*, vol. 9, no. 2, pp. 195–211, Jan. 2020.

FUAD S. ALDUAIS received the Ph.D. degree from Damascus University, Syria, in 2009. He is currently an Associate Professor with the Department of Mathematics, College of Science and Humanities, Prince Sattam bin Abdulaziz University, Saudi Arabia. His research interests include reliability estimation, Bayesian inference, survival analysis, probability distributions, applied statistics, and control chart theory.

ZAHID KHAN received the Ph.D. degree from University Technology PETRONAS, Malaysia, in 2017. He is currently an Assistant Professor with the Department of Mathematics and Statistics, Hazara University Mansehra, Pakistan. His research interests include robust estimation in fuzzy probability distributions, neutrosophic statistics, and statistical methods for industrial process control. He was a recipient of the Talent Award Scholarship from the Higher Education Commission of Pakistan, in 2006; a Fellowship from Quaid-i-Azam University, in 2007; and a Fellowship from University Technology PETRONAS, in 2013.